# The *C. elegans* proteome response to two protective *Pseudomonas* symbionts

Barbara Pees[a*], Lena Peters[a], Christian Treitz[b], Inga K. Hamerich[a], Kohar A. B. Kissoyan[a], Andreas Tholey[b], Katja Dierking[a*]

[a]Department of Evolutionary Ecology and Genetics, Zoological Institute, Christian-Albrecht University, Kiel, Germany

[b]Systematic Proteome Research & Bioanalytics, Institute for Experimental Medicine, Christian-Albrecht University, Kiel, Germany

*Correspondence: bpees@zoologie.uni-kiel.de, kdierking@zoologie.uni-kiel.de

**Running title**

**A proteomic view on *C. elegans*-microbiota interactions**

## Abstract

The *C. elegans* natural microbiota isolates *Pseudomonas lurida* MYb11 and *Pseudomonas fluorescens* MYb115 protect the host against pathogens through distinct mechanisms. While *P. lurida* produces an antimicrobial compound and directly inhibits pathogen growth, *P. fluorescens* MYb115 protects the host without affecting pathogen growth. It is unknown how these two protective microbes affect host biological processes. We used a proteomics approach to elucidate the *C. elegans* response to MYb11 and MYb115. We found that both *Pseudomonas* isolates increase vitellogenin protein production in young adults, which confirms previous findings on the effect of microbiota on *C. elegans* reproductive timing. Moreover, the *C. elegans* responses to MYb11 and MYb115 exhibit common signatures with the response to other vitamin $B_{12}$-producing bacteria, emphasizing the importance of vitamin $B_{12}$ in *C. elegans*-microbe metabolic interactions. We further analyzed signatures in the *C. elegans* response specific to MYb11 or MYb115. We provide evidence for distinct modification in lipid metabolism by both mutualistic microbes. We could identify activation of host pathogen defense responses as MYb11-specific proteome signature and demonstrate that the intermediate filament protein IFB-2 is required for MYb115-mediated protection. These results indicate that MYb11 not only produces an antimicrobial compound, but also activates host antimicrobial defenses, which together might increase resistance to infection. In contrast, MYb115 affects host processes such as lipid metabolism and cytoskeleton dynamics, which might increase host tolerance to infection. Overall, this study provides new insights into the potential mechanisms underlying *C. elegans* microbiota-mediated protection from pathogen infection.

# Introduction

In line with the growing general interest in host-microbiota interactions, *Caenorhabditis elegans* has emerged as a model host to study the effect of different food and benign bacteria on host metabolism and physiology. The bacteria used in these studies include bacteria that likely are associated with nematodes in their habitat, such as *Comamonas aquatica*, *Bacillus subtilis*, and different *Escherichia coli* strains (reviewed in (1)), and probiotic bacteria of human origin such as *Lactobacillus* and *Bifidobacterium* (reviewed in (2)). The characterization of the *C. elegans* natural microbiome (3, 4) and the creation of the simplified natural nematode microbiota mock community CeMBio (5) initiated a steadily increasing number of recent studies on naturally associated microbes and their interaction with the nematode (reviewed in (4, 6)). While we still know relatively little about the function of the *C. elegans* natural microbiota, several studies underline an important role of the microbiota in supporting the nematode immune response (e. g. (3, 7–9)).

We previously identified two *Pseudomonas* isolates of the natural *C. elegans* microbiota, which protect the worm from infection with *Bacillus thuringiensis* (Bt) through different mechanisms: While *P. lurida* MYb11 produces the antimicrobial secondary metabolite massetolide E and directly inhibits pathogen growth, *P. fluorescens* MYb115 does not seem to directly inhibit pathogen growth and may thus protect the host by indirect, host-dependent mechanisms (9). Also, while the known effects of MYb115 on *C. elegans* survival, lifespan and fertility are either beneficial or neutral, MYb11 has pathogenic potential in some contexts. For example, MYb11 reduces lifespan and aggravates killing upon exposure to purified Bt toxins (10). Thus, colonization of *C. elegans* by these two microbes seems to have wide-ranging effects on host physiology.

*C. elegans* responses to different food bacteria and natural microbiota isolates have been investigated mainly by transcriptome analyses (e. g. (11–15)) and only a few proteome analyses (16, 17). Here, we analyzed the direct effects of the protective Pseudomonads MYb11 and MYb115 on the *C. elegans* proteome. To this end, we employed quantitative proteomics and analyzed both, commonalities and differences, in the *C. elegans* proteomic response to MYb11 and MYb115 and validated some of the findings using qRT-PCR, reporter genes, or mutant analyses. We found that both *Pseudomonas* isolates impact *C. elegans* reproductive timing by increasing vitellogenin protein production in young adults. Furthermore, the responses to MYb11 and MYb115 show similarities with responses to other vitamin $B_{12}$-producing bacteria, such as *Ochrobactrum* and *Comamonas*, highlighting the significance of vitamin $B_{12}$ in *C. elegans*-microbe metabolic interactions. Our analysis of the *C. elegans* response to MYb11 and MYb115 reveals specific modifications in lipid metabolism. Additionally, we found that MYb11 activates host pathogen defense responses and that the intermediate filament protein IFB-2 is required for MYb115-mediated protection. These results suggest that MYb11 activates host antimicrobial defenses in addition to producing an antimicrobial compound, potentially increasing resistance to infection, while MYb115 improves host tolerance to infection by affecting lipid metabolism and other host processes. With our findings we contribute to the understanding of the different molecular mechanisms that underlie host-microbiota interactions particularly in the context of microbiota-mediated protection against pathogens.

# Materials & Methods

## Strains, maintenance, and preparations

Wild type *C. elegans* N2 and all used *C. elegans* mutants/transgenics, as well as bacteria control *Escherichia coli* OP50, were received from sources indicated in Table S1 and maintained according to standard procedures (18). For experiments, worms were synchronized by bleaching gravid hermaphrodites with alkaline hypochlorite solution and incubating the eggs in M9 overnight on a shaker.

Spore solutions of pathogenic *Bacillus thuringiensis* strain MYBt18247 (Bt247) were prepared following a previously established protocol (19), and stored at -20 °C. Single aliquots were freshly thawed for each inoculation.

*Pseudomonas lurida* MYb11 and *Pseudomonas fluorescens* MYb115 belong to the natural microbiota of *C. elegans* (3) and were kept frozen in glycerol stocks at -80 °C. Before each experiment, bacterial strains were streaked from glycerol stocks onto TSB agar plates, grown for 2 days at 25 °C, and consequently for an overnight in TSB at 28 °C. On the day before adding the worms, bacteria of the overnight cultures were harvested by centrifugation, resuspended in 1x PBS, pH7, adjusted to an $OD_{600}$ of 10, and used for inoculation of peptone-free medium (PFM, nematode growth medium without peptone) plates.

## qRT-PCR

Worms were raised on OP50, MYb11, or MYb115 until they reached young adulthood, 70 h after synchronized L1s were transferred to the plates. For each replicate roughly 1,000 worms were washed off the plates with 0.025% Triton X-100 in M9 buffer along with three gravity washing steps. Freezing and RNA isolation was done following the instructions of the NucleoSpin RNA/Protein Kit (Macherey-Nagel; Düren, Germany). 1 µg of the extracted total RNA per sample was reverse transcribed using oligo(dt)18 primers (First Strand cDNA Synthesis Kit; Thermo Scientific; Waltham, USA), and 1 µL cDNA was used for qRT-PCR with *tgb-1* as housekeeping gene (20). The expression levels of all tested primers were determined using the iQ™ SYBR® Green Supermix (Bio-Rad, Hercules, USA) using the settings as suggested in the manual. Primer sequences are to be found in Table S2. The $2^{-\Delta\Delta Ct}$ method was used to calculate the relative gene expression (21).

## Survival experiments and imaging

Synchronized L1 larvae were grown on PFM plates prepared with lawns of OP50, MYb11, or MYb115 at 20 °C as described above. PFM infection plates were inoculated with serial dilutions of Bt spores mixed with bacterial OP50, MYb11, or MYb115 solutions. As L4s, worms were rinsed off the plates and washed with M9, and pipetted in populations of approx. 30 individuals on each Bt infection plate. After 24 h incubation at 20 °C survival of worms was scored. Worms were considered to be alive when they moved upon gentle prodding with a worm pick. Replicates with less than 15 worms at the time of scoring were excluded.

For imaging of *in vivo* gene/protein expression, transgenic worms were treated as for survival experiments but without Bt infection. Young adults (24 h post L4) were then anesthetized with 10 mM tetramisole, placed onto a fresh 2 % agarose patch, and imaged with a Leica stereomicroscope M205 FA (Wetzlar,

Germany). Magnification and exposure time for the fluorophore signal were kept the same in each experiment to ensure comparability. Final editing of the images was done with ImageJ v1.53t (22).

## Proteome analysis

Worms for proteomic analyses were grown on PFM plates prepared with lawns of OP50, MYb11, or MYb115 at 20 °C as described above. L4 stage larvae were transferred to freshly inoculated PFM plates to provide sufficient food. Approx. 1,500 worms per replicate were harvested at 12 h post L4 and washed across a Steriflip® 20 µm nylon mesh filter (Merck; Darmstadt, Germany) with M9 buffer. The samples were prepared as four independent biological replicates.

To each sample, 200 µL protein lysis buffer (100 mM triethylammonium bicarbonate TEAB, 2% SDS, 5 M guanidinium chloride, 2 mM dithiothreitol DTT; 2x complete protease inhibitor) and approx. 200 µL of acid washed glass beads were added. The samples were homogenized using a Bioruptor pico for 20 cycles of 30 s sonication and 30 s cooling at 4 °C. The protein concentration was determined by BCA assay. The proteins were reduced with 10 mM DTT for 1 h at 60 °C and alkylated with 25 mM chloroacetamide at 20 °C for 20 min. The samples were centrifuged for 10 min at 10,000 g and aliquots of 100 µg were prepared following the SP3 protocol (23).

A detailed description of the LC-MS analysis is provided in Supplemental Materials and Methods. Briefly, for each of the 12 samples, approximately 1 µg of peptides were analyzed by liquid chromatography-electrospray ionization-mass spectrometry (LC-ESI MS/MS). Proteome digests were separated over a 2 h gradient on a 50 cm C18 nano-uHPLC column and high-resolution mass spectra were acquired with an Orbitrap Fusion Lumos mass spectrometer. Proteome Discoverer software and the Sequest algorithm were used for peptide identification and label-free quantification. MS data were searched against the reference proteome of *C. elegans* (26,738 entries) combined with the UniParc entries of *P. lurida* (5,392 entries), *P. fluorescens* (5,548 entries), and *E. coli* OP50 (4,227 entries). Statistical evaluation of the quantitative data was performed with the Perseus software (24). LC-MS raw data were deposited to the ProteomeXchange Consortium via the PRIDE partner repository (25) with the dataset identifier PXD040520.

## Statistical analyses

For identification of differentially abundant proteins, we performed a one-way ANOVA comparing the three conditions (OP50 *vs* MYb11 *vs* MYb115) and corrected for multiple comparisons using a permutation-based FDR analysis. An FDR cut-off of 5% was applied and Tukey's HSD test was used for *post hoc* analysis. Significant protein groups assigned to each of the pairs of conditions were tested for UniProt keywords by Fisher exact test corrected for multiple testing by Benjamini-Hochberg FDR calculation. All significant findings with an FDR below 5% are provided in Table S3.

Heatmaps were created using the Morpheus (https://software.broadinstitute.org/morpheus), GO term overrepresentation analyses were done with eVitta v1.3.1 (26). All remaining statistical analyses were carried out with RStudio, R v4.2.1, graphs created with its package ggplot2 v3.3.6 (27), and edited with Inkscape v1.1.2.

# Results & Discussion

## Common proteomic response to protective *Pseudomonas*.

We were interested in identifying the proteomic changes in *C. elegans* exposed to two beneficial, protective *Pseudomonas* strains, *P. lurida* MYb11 and *P. fluorescens* MYb115. To this end, worms were grown on MYb11, MYb115, or *E. coli* OP50 and harvested for proteome analysis as young adults. Using LC-MS analysis we identified 4,314 protein groups in total, which included 259 protein groups annotated to bacterial taxa and 4,055 to *C. elegans* protein groups. For statistical evaluation, the identified *C. elegans* proteins were filtered to 3,456 entries quantified in all four replicates of at least one bacterial treatment. The complete list of proteins is provided in Table S3.

674 proteins were differentially abundant in MYb-treated worms compared to OP50-treated worms, 201 proteins out of these 674 proteins were differentially abundant in both comparisons, MYb11 *vs* OP50 and MYb115 *vs* OP50 (Figure 1A; Table S3). When we grouped the shared proteomic response towards *Pseudomonas* into more and less abundant proteins, we obtained 84 higher abundant proteins and 104 less abundant proteins (Figure 1B, C). Strikingly, among the more abundant proteins we found all six vitellogenins described in *C. elegans* (28, 29). Vitellogenins are yolk proteins which are primarily produced in the reproductive phase to supply energy to the embryos (30). Expression of the vitellogenins encoding *vit* genes is known to be greatly up-regulated in young adults and down-regulated in aging worms (31). We have previously shown that MYb11 and MYb115 accelerate *C. elegans* reproductive maturity (10). Thus, it might be possible that the abundance of vitellogenins in worms treated with either of the Pseudomonads reflects these differences in reproductive maturity. When we compared the abundance of the vitellogenin VIT-2 between young adults on MYb11, MYb115, or OP50 using a *C. elegans vit-2*::gfp reporter strain, we indeed observed an increased number of eggs and VIT-2 abundance in worms on MYb11 and MYb115 (Figure 1B). This observation is reminiscent of data on *Comamonas aquatica* DA1877 and *Enterobacter cloacae* CEent1 that accelerate *C. elegans* development (7, 11). In addition to their function in energy supply for the developing embryo, vitellogenins play a role in pathogen defenses. In the honey bee vitellogenin drives transgenerational immune priming by binding pathogen-associated molecular patterns of e. g. *E. coli* and by transporting these signals into developing eggs (32). Also, in *C. elegans* vitellogenins are involved in defense against *Photorhabdus luminescens* (33). Even more relevant, VIT-2 is required for *Lactobacillus*-mediated protection against Methicillin-resistant *Staphylococcus aureus*, albeit in aging worms (17). Taken together, the enhanced production of *C. elegans* vitellogenins in response to *Pseudomonas* microbiota might reflect differences in reproductive timing, but could also play a role in the protective effects mediated by MYb11 and MYb115 against pathogens. Whether *C. elegans* vitellogenins affect MYb11-and MYb115-mediated protection against pathogens is an interesting question for future work.

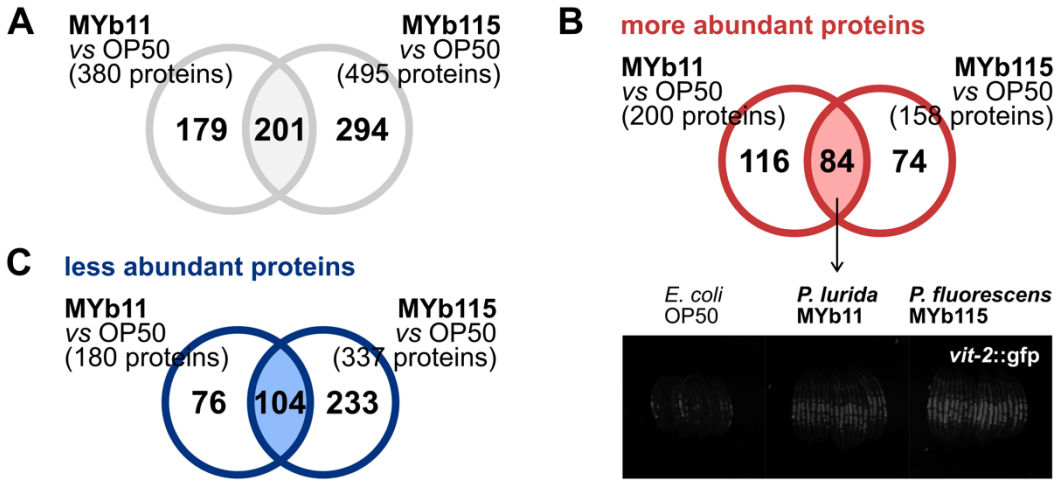


**Figure 1. Proteomic response of *C. elegans* towards mutualistic *Pseudomonas*.** Venn diagrams showing (A) all significantly differentially abundant proteins resulting from comparing either MYb11-exposed worms to OP50-exposed worms or MYb115-exposed worms to OP50-exposed worm, (B) only the significantly more abundant proteins, or (C) the significantly less abundant proteins; ANOVA, *post hoc* Tukey HSD, $p > 0.05$. (B) Transgenic *C. elegans* reporter strain *vit-2*::gfp demonstrating *in vivo* abundance of VIT-2. Worms were exposed to either *E. coli* OP50, *P. lurida* MYb11, or *P. fluorescens* MYb115, and GFP signals imaged in groups of 20 individuals as young adults. Worms were arranged with the heads pointing upwards.

## Microbiota bacteria elicit a robust proteomic response related to vitamin $B_{12}$-dependent metabolism.

*Pseudomonas* and *Ochrobactrum* represent the most prevalent genera in the natural *C. elegans* microbiota, are able to colonize the host, and seem to have largely beneficial effects on host life-history traits (3–5, 9, 34). We previously analyzed the effects of *O. vermis* MYb71 and *O. pseudogrignonense* MYb237 on the *C. elegans* proteome (16). Here, we asked whether the *C. elegans* proteome response to the Pseudomonads MYb11 and MYb115 shares common signatures with the response to *O. vermis* MYb71 and *O. pseudogrignonense* MYb237. We extracted significantly differentially abundant proteins in either MYb71 *vs E. coli* OP50 or MYb237 *vs E. coli* OP50 from the published dataset, and examined the overlap between responses to all four microbiota isolates. We identified 32 proteins, whose abundances were affected by all four microbiota bacteria (Figure 2A, Table S4). 31 of the 32 proteins showed a common increase and decrease in abundances, respectively, relative to the control *E. coli* OP50. One protein, the uncharacterized CHK domain-containing protein F58B4.5 (Table S4), was more abundant in worms fed with either *Ochrobactrum* strains but less abundant on *Pseudomonas*. It thus represents a promising candidate for understanding contrasting responses to both taxa. We further noticed that 11 proteins out of the 31 proteins representing the common proteome response to *Pseudomonas* and *Ochrobactrum* are members of the interacting methionine/S-adenosylmethionine (met/SAM) cycle, which is part of the one-carbon cycle, and the alternative propionate shunt pathway (35, 36) (Figure 2B). In this signaling network, vitamin $B_{12}$ is a crucial micronutrient that feeds into methionine synthesis and allows the breakdown of propionate (35, 37), thereby promoting *C. elegans* longevity, fertility, development, and mitochondrial health (38, 39). The importance of microbial-derived vitamin $B_{12}$ in regulating the host met/SAM cycle has previously been demonstrated by comparing a *C. aquatica* DA1877 diet, which is naturally rich in vitamin

$B_{12}$, to the standard *C. elegans* food *E. coli* OP50 (35). Similarly, both *Ochrobactrum* strains, MYb71 and MYb237, and both *Pseudomonas* strains, MYb11 and MYb115, are predicted vitamin $B_{12}$ producers (34).

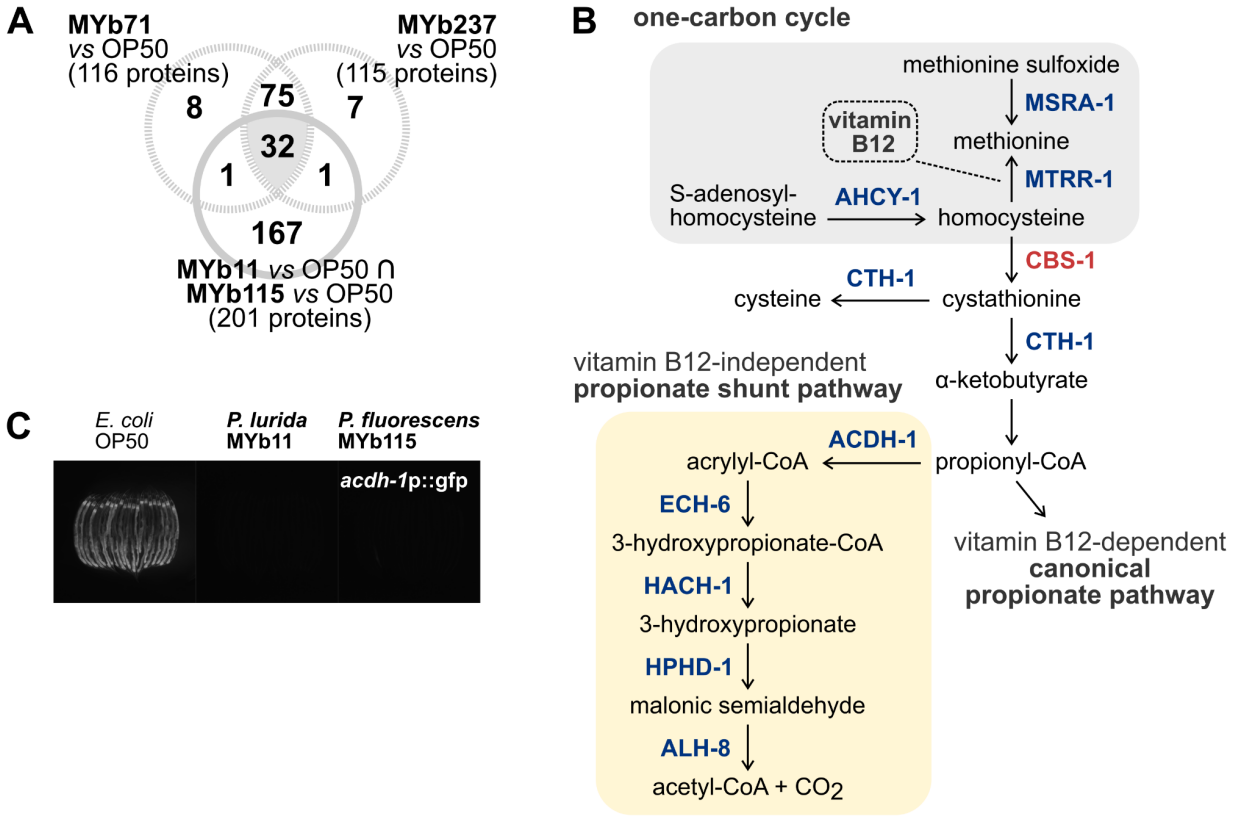


**Figure 2. Changes in vitamin $B_{12}$-dependent metabolism are shared proteomic responses to mutualistic *Pseudomonas* and *Ochrobactrum*.** (A) Venn diagram showing all significantly differentially abundant proteins resulting from the overlap of the comparison MYb11 *vs* OP50 and MYb115 *vs* OP50 (Figure 1A) compared against differentially abundant proteins on *Ochrobactrum* MYb71 and MYb237. (B) Excerpt of the one-carbon cycle (gray background) and the propionate pathways (yellow background). Shown are mainly the steps which involve commonly differentially abundant proteins in worms grown on mutualistic *Pseudomonas* and *Ochrobactrum*. Protein coloring depicts either less abundant (blue) or more abundant (red) proteins. CoA = coenzyme A. Adapted from (35, 36). (C) Transgenic *C. elegans* reporter strain *acdh-1*p::gfp demonstrating *in vivo* expression of *acdh-1*. Worms were exposed to either *E. coli* OP50, *P. lurida* MYb11, or *P. fluorescens* MYb115, and GFP signals imaged in groups of 20 individuals as young adults. Worms were arranged with the heads pointing upwards.

In the presence of vitamin $B_{12}$ *C. elegans* uses the canonical propionate pathway to degrade propionate into less toxic metabolites and, simultaneously, inactivates the $B_{12}$-independent propionate shunt, i. e. by down-regulating the partaking genes (35, 40) (Figure 2B). Exactly these propionate shunt proteins, ACDH-1, ECH-6, HACH-1, HPHD-1, and ALH-8, were less abundant in the microbiota-treated worms which is further evidence for the provision of vitamin $B_{12}$ by *Pseudomonas* and *Ochrobactrum*. Also, genes encoding the 12 proteins that show different abundances by *Pseudomonas* and *Ochrobactrum* (Table S4), were reported to be differentially regulated by either *C. aquatica* DA1877 or vitamin $B_{12}$ supplementation (35, 36, 41). We confirmed that expression of the acyl-CoA dehydrogenase encoding gene *acdh-1* is down-

regulated by MYb11 and MYb115 by using the dietary sensor *C. elegans* strain *acdh-1*p::gfp, which reacts to vitamin $B_{12}$ presence (35, 42) (Figure 2C). Thus, the robust, shared proteomic response of *C. elegans* to mutualistic *Pseudomonas* and *Ochrobactrum* seems to be driven by the availability of vitamin $B_{12}$ and subsequent metabolic signaling. Interestingly, increased vitamin $B_{12}$ availability was shown to improve *C. elegans* mitochondrial health and resistance to infection with *P. aeruginosa* and *Enterococcus faecalis* in a liquid-based killing assay, but not to *P. aeruginosa*-mediated slow killing (39). Furthermore, increased vitamin $B_{12}$ availability protects *C. elegans* against exposure to the thiol-reducing agent dithiothreitol (43). These and other findings stress the central importance of dietary vitamin $B_{12}$ in *C. elegans* metabolic processes and reveal roles of vitamin $B_{12}$ in the regulation of growth, development, lifespan, chemosensory receptor gene expression, and responses to stress (11, 38, 44, 45). The possibility of a role of vitamin $B_{12}$ in MYb11- and MYb115-mediated protection against pathogen infection warrants further investigation.

## Proteomic responses of *C. elegans* specific to MYb11 and MYb115.

While both Pseudomonads, MYb11 and MYb115, are able to protect *C. elegans* from Bt infection, the underlying mechanisms are distinct (9). MYb11-mediated pathogen protection against Bt seems to rely primarily on direct inhibition of pathogen growth through the production of the cyclic lipopeptide massetolide E. In contrast, MYb115 does not inhibit pathogen growth and MYb115-mediated pathogen protection, thus, likely relies on indirect, host-dependent mechanisms (9). As a step toward understanding the contribution of the host response to MYb11- and MYb115-mediated protection, we sought to identify the differences in the proteomic responses between worms exposed to MYb11 and MYb115. Both treatments were directly compared and we found 421 proteins that differed significantly in their abundance between the two conditions (Figure 3A). Interestingly, 326 proteins were more abundant in worms grown on MYb11 compared to MYb115 and only 95 proteins were more abundant in MYb115-exposed worms compared to MYb11-exposed worms (Figure 3A). To extract the proteins that were uniquely differently abundant in either MYb11 or MYb115, we included the data on OP50 to generate 4 clusters using *k*-means clustering: cluster 1 and 4 represent proteins whose abundance only changed in MYb11-exposed worms, i. e. in reference to MYb115 and OP50, while cluster 2 and 3 represent proteins with different abundances specifically in MYb115-exposed worms, i. e. in reference to MYb11 and OP50, (Figure 3A). Next, we employed eVitta, an online tool developed for the analysis and visualization of transcriptome data (26), to look for enriched gene ontology (GO) terms in these clusters.

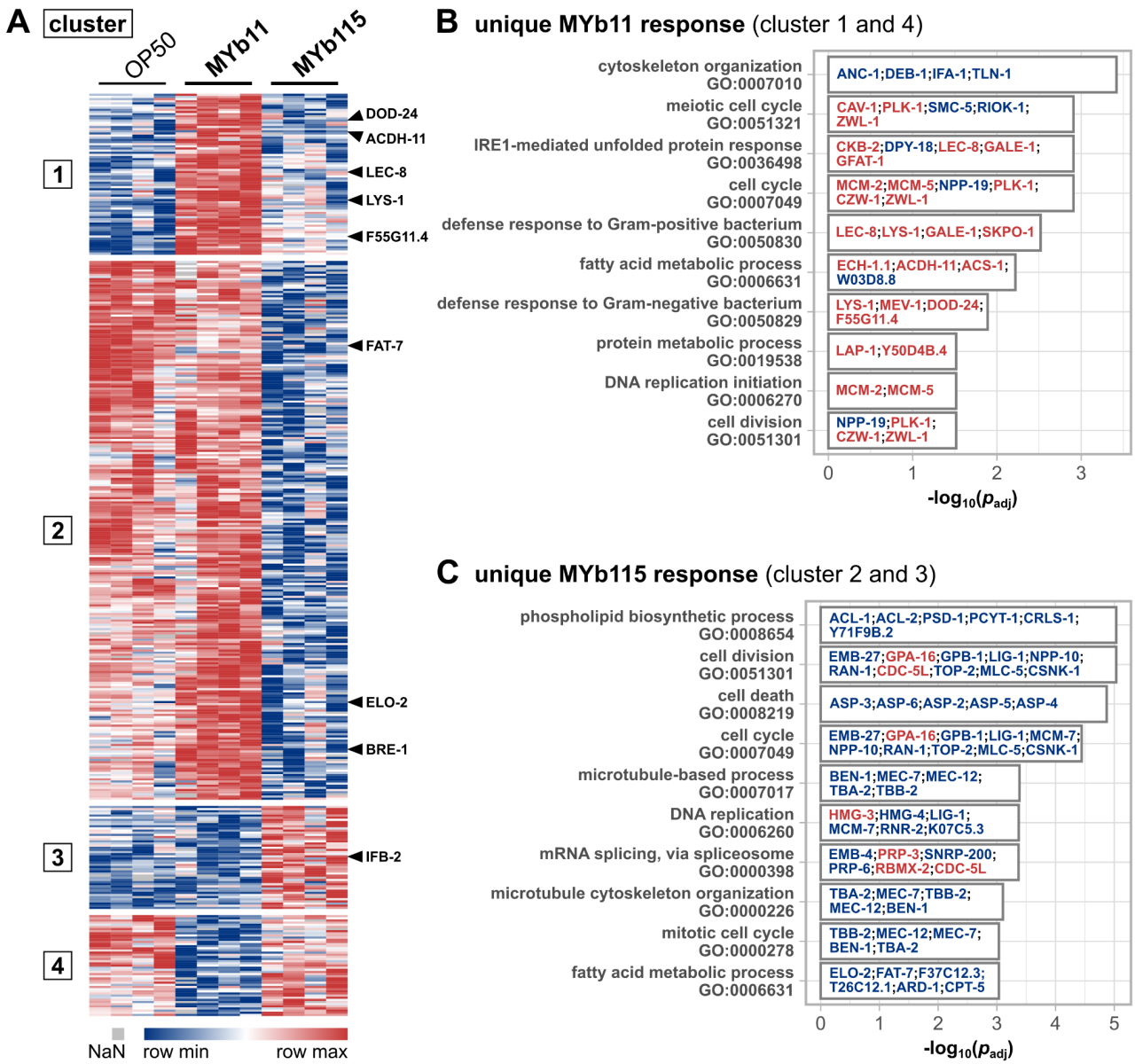


**Figure 3. Differences in the proteomic responses of *C. elegans* towards *P. lurida* MYb11 compared to *P. fluorescens* MYb115.** (A) Heatmap showing the $\log_2$ label-free intensity values of differentially abundant proteins in the comparison of MYb11-exposed worms against MYb115-exposed worms. The columns denote the bacterial treatment with 4 replicates each, each row represents one protein. By including the data on OP50, abundance values were separated into 4 clusters using the *k*-means clustering approach. The rows of exemplary proteins mentioned in the text are marked on the heatmap's right. Bar plot of significantly enriched gene ontology (GO) terms in either (B) clusters 1 and 4 (different abundances of proteins uniquely in MYb11-treated worms) or (C) clusters 2 and 3 (different abundances of proteins uniquely in MYb115-treated worms). The proteins which are assigned to the respective GO term are noted on the bars, their coloring indicates higher (red) or lower (blue) abundance. Shown are the 10 GO terms with the highest significance. The complete list of GO terms is to be found in Tables S5 and S6.

## MYb11 causes a mild pathogen response in *C. elegans*.

Proteins affected by both *Pseudomonas* isolates were enriched in GO terms associated with nucleic acids (e. g., DNA replication, mRNA splicing), and also fatty acid-related terms albeit targeting different fat metabolism enzymes (see below). On the contrary, defense response proteins were a MYb11-linked feature with defense responses to Gram-positive bacterium (GO:0050830) and Gram-negative bacterium (GO:0050829) among the 10 highest significantly enriched GO terms in the unique MYb11 response (Figure 3B, Table S3). Interestingly, the 7 proteins (LYS-1, LEC-8, GALE-1, SKPO-1, MEV-1, DOD-24, F55G11.4) associated with the GO defense response terms were all more abundant in MYb11 compared to MYb115, indicating that MYb11 induces *C. elegans* pathogen defenses while MYb115 does not. This finding is in line with the previous observation that MYb11 has a pathogenic potential in some contexts, despite its protective effect against Bt and *P. aeruginosa*, resulting in a shorter lifespan and increased susceptibility to purified Bt toxins (10). Hence, we assessed the general pathogenicity of MYb11 and tested activation of the *C. elegans* stress reporters, *hsp-4*::gfp (endoplasmic reticulum stress), *hsp-6*::gfp and *hsp-60*::gfp (mitochondrial stress (46, 47)), *gst-4*p::gfp (oxidative stress (48)), and the immune reporters *irg-1*p::gfp (49) and *clec-60*p::gfp (50). Bacteria from the natural *C. elegans* habitat were reported to induce expression of some of these reporter genes (51). We found that the oxidative stress reporter *gst-4*p::gfp was up-regulated by MYb11 and less strongly by MYb115 (Figure 4A). MYb11, but not MYb115, also slightly induced expression of the C-type lectin-like gene *clec-60* reporter. These results indicate that MYb11 activates the *C. elegans* oxidative stress response and the expression of specific defense response genes. To explore in how far the *C. elegans* proteome response to MYb11 overlaps with the proteome response to pathogenic bacteria, we compared our data (Figure 1B) with the proteomic changes elicited by pathogenic *P. aeruginosa* PA14 (52) and Bt247 (53). The comparison of proteins of higher abundance in MYb11-exposed worms with PA14-responsive proteins yielded an overlap of 14 more abundant proteins (Figure 4B). Among these 14 proteins were the CUB-like domain proteins C17H12.8, C32H11.4, DOD-17, DOD-24 and F55G11.4 and the infection response gene (IRG) 3. Similarly, when we compared the response to MYb11 to the proteomic response to Bt infection, the abundances of 11 proteins were commonly increased (Figure 4C). Among these proteins were the CUB-like domain proteins C17H12.8, the lysozyme LYS-1, the galectins LEC-8 and LEC-9, and the C-type lectin-like domain proteins CLEC-41 and CLEC-65. Lysozymes are required for resistance against Bt247 (54) and the galectin LEC-8 (Figure 3B) protects *C. elegans* from *B. thuringiensis* toxin *Cry5B* by competitively binding to glycolipids, that function as Cry toxin targets (55). CLEC-41 is a *C. elegans* immune effector protein that exhibits antimicrobial activity against Bt247 (56).

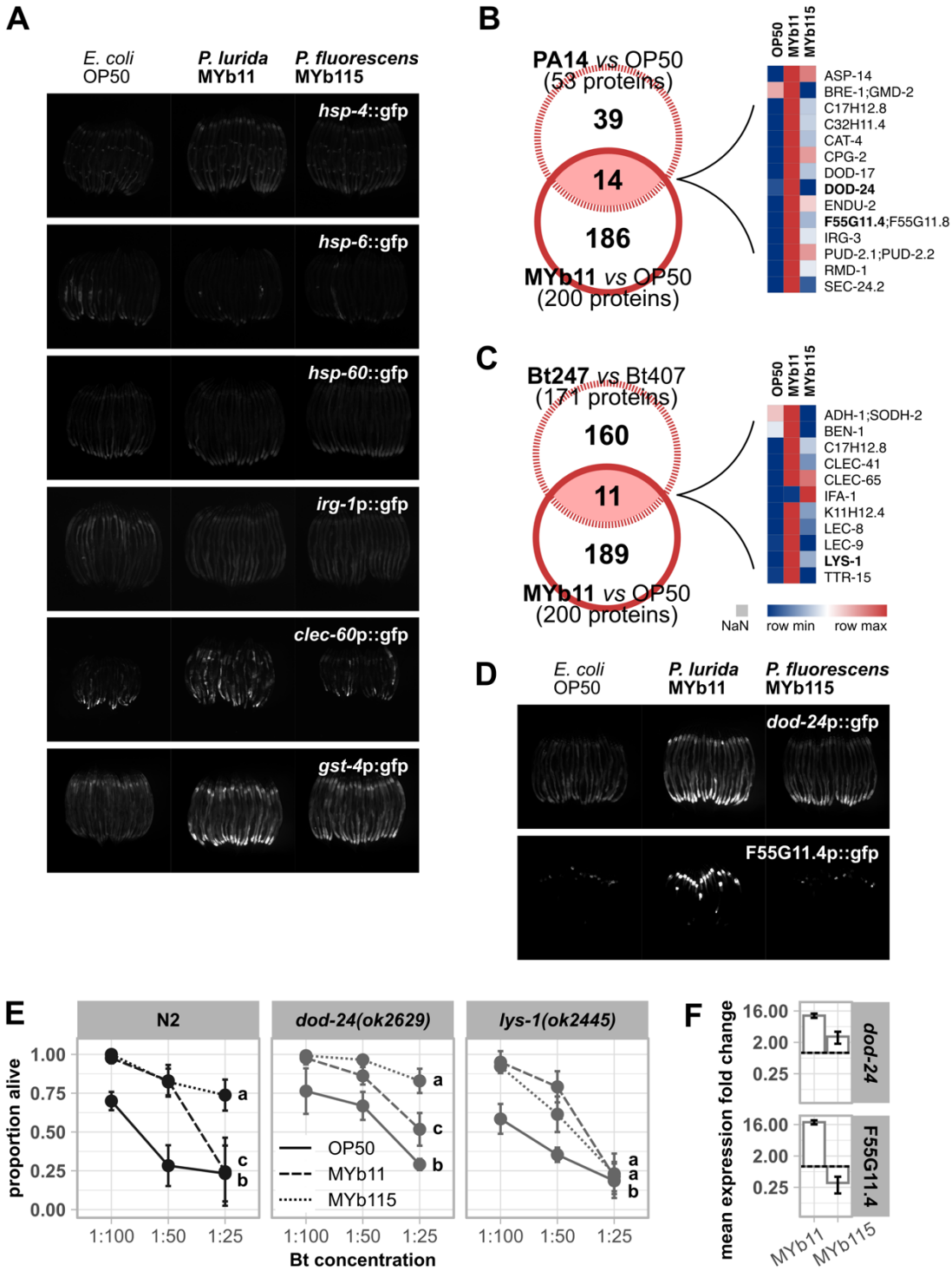


**Figure 4. MYb11 activates expression of *C. elegans* innate immune response genes and proteins.** (A, D) Transgenic *C. elegans* reporter strains demonstrating *in vivo* expression of selected genes/promotor sequences tagged with GFP. Transgenic strains were exposed to either *E. coli* OP50, *P. lurida* MYb11, or *P. fluorescens* MYb115, and fluorescent signals imaged in groups of 20 individuals as young adults. Worms were arranged with the heads pointing upwards. Venn diagrams showing significantly more abundant proteins resulting from the comparison MYb11 *vs* OP50 (Figure 1B) compared against significantly more abundant proteins of (B) *P. aeruginosa* PA14, and (C) *B. thuringiensis* Bt247. The accompanying heatmaps represent the averaged $\log_2$ label-free intensity values ($n$ = 4) of the overlapping significant proteins. Data taken from (52, 53). (E) Survival of *dod-24(ok2629)*, *lys-*

*1(ok2445)*, and N2 infected with serial dilutions of *B. thuringiensis* Bt247 after 24 hpi (post infection). Worms were exposed to either OP50, MYb11, or MYb115 before and during infection. Means ± standard deviation (SD) of $n = 4$ are shown. Same letters indicate no significant differences between the dose response curves according to a generalized linear model (GLM) (57) and Bonferroni correction. Corresponding *p*-values are provided in Table S7. (F) Expression of *dod-24* and F55G11.4 in worms exposed to either MYb11 or MYb115 in relation to worms fed with OP50 (depicted as dashed line) measured with qRT-PCR. Means ± standard deviation (SD) of $n = 2$ are shown.

Although MYb11 produces the antimicrobial secondary metabolite massetolide E and directly inhibits pathogen growth (9), activation of host pathogen defense responses, i. e. production of host immune proteins, may contribute to MYb11-mediated protection. To explore this possibility, we focused on DOD-24 and F55G11.4, whose abundances were strongly increased by MYb11; F55G11.4 being the protein with the highest abundance on MYb11 (Table S3). First, using qRT-PCR and GFP reporter gene promoters, we confirmed that expression of *dod-24* and *F55G11.4* is up-regulated by MYb11 in comparison to MYb115 or OP50 also on the transcript level (Figure 4D, F). To determine if MYb11-induced genes have a function in MYb11-mediated protection against Bt infection we grew *lys-1* and *dod-24* knock-out mutants on OP50, MYb11, or MYb115, infected them with Bt247, and scored their survival. MYb11 and MYb115 increased resistance to Bt247 infection also in *lys-1* and *dod-24* mutants (Figure 4E). Thus, DOD-24 and LYS-1 may be functional redundant to other effectors so that knock-out of individual genes does not have an effect or they are not critical for MYb11-mediated protection against Bt247 infection. However, work on other protective microbes support our findings on the ability of MYb11 to induce *C. elegans* pathogen defenses. For example, *L. acidophilus*, which protects *C. elegans* against infection with *E. faecalis* and *S. aureus*, up-regulates expression of specific defense response genes, including *clec-60*, but not *dod-24* or C17H12.8 (58). *E. faecium* that provides protection against *Salmonella enterica* infection activates expression of antimicrobial peptide genes such as *ilys-3* (59). Further studies are necessary to clarify if the effect of MYb11 on potential host immune effector proteins contributes to MYb11-mediated protection against pathogens.

Notably, most of the innate immune response proteins that showed an increased abundance on MYb11, did not show higher abundances on MYb115 (Figure 3). Similarly, MYb11, but not MYb115 induced expression of the *clec-60*p::gfp reporter. This is an interesting finding since *clec-60*p::gfp expression is induced by pathogenic *S. aureus*, but not by *P. aeruginosa* PA14 (60). Also, intestinal lumen bloating by bacterial colonization induces *clec-60*p::gfp expression (61). Our results however suggest that colonization of the worm by mutualistic microbes such as MYb11 and MYb115 *per se* does not activate *C. elegans* pathogen defenses or that certain bacteria are able to inhibit the bloating-induced immune response. It remains to be determined if and how MYb115 inhibits activation of *C. elegans* immune response genes.

## MYb11 and MYb115 cause diverging responses in *C. elegans* fat metabolism.

Among the 10 highest significantly enriched GO terms concerning biological processes in the unique MYb11 response as well as in the unique MYb115 response, we found the term fatty acid metabolic process (GO:0006631) (Figure 3B, C). Moreover, the GO term phospholipid biosynthetic process (GO:0008654) was enriched only in the unique MYb115 response (Figure 3C). Since the ability to mount an immune response has been repeatedly linked to changes in *C. elegans* fat metabolism (e. g. (62, 63)), we took a closer look at the underlying proteins. While the predicted fatty acid β-oxidation enzyme ECH-1.1, the acyl-CoA dehydratase ACDH-11, and the acyl-CoA synthetase ACS-1 were of higher abundance in

worms on MYb11 (Figure 3B, Table S3), the fatty acid elongase ELO-2 and the fatty acid desaturase FAT-7 were of lower abundance in worms on MYb115 (Figure 3C, Table S3). FAT-6 and FAT-7 are members of the long-chain fatty acid synthesis pathway and act redundantly in the synthesis of the monounsaturated fatty acid oleate from stearic acid (64). Interestingly, oleate is required for the activation of *C. elegans* pathogen defenses against infection with *E. faecalis*, *Serratia marcescens*, and *P. aeruginosa* (63). We thus validated the effect of the *Pseudomonas* isolates on FAT-7 by assessing the *in vivo* protein abundance of *fat-7*::gfp in worms exposed to *E. coli* OP50, *P. lurida* MYb11, or *P. fluorescens* MYb115. Expression of *fat-7*::gfp was indeed reduced in worms on MYb115 compared to worms on OP50 or MYb11 (Figure 5A), confirming that MYb11 and MYb115 cause diverging responses in *C. elegans* fat metabolism.

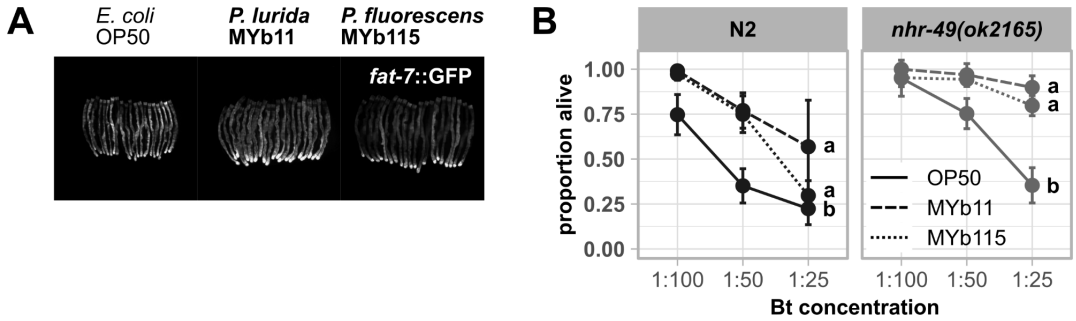


**Figure 5. Divergent proteomic changes in fat metabolism occur in MYb11- and MYb115-exposed worms but common fat metabolism regulator NHR-49 is not involved in the defense against Bt247 infection.** (A) Transgenic *C. elegans* reporter strain demonstrating *in vivo* abundance of FAT-7. Worms were exposed to either *E. coli* OP50, *P. lurida* MYb11, or *P. fluorescens* MYb115, and GFP signals imaged in groups of 20 individuals as young adults. Worms were arranged with the heads pointing upwards. (B) Survival of *nhr-49(ok2165)* and N2 infected with serial dilutions of *B. thuringiensis* Bt247 after 24 hpi. Worms were fed with either OP50, MYb11, or MYb115 before and during infection. Means ± standard deviation (SD) of $n = 4$ are shown. Same letters indicate no significant differences between the dose response curves according to a generalized linear model (GLM) (57) and Bonferroni correction. Corresponding *p*-values are provided in Table S7.

The nuclear hormone receptor NHR-49 is a major regulator of *C. elegans* fat metabolism and activates *fat-7* expression (65). NHR-49 also mediates *C. elegans* defenses against infection with *E. faecalis* (62), *P. aeruginosa* (66), and *S. aureus* (67). Thus, we first evaluated the role of *nhr-49* in the protective effect mediated by either *Pseudomonas* strain. We tested the survival of the knock-out mutant *nhr-49(ok2165)* infected with Bt in the presence of either OP50, MYb11, or MYb115. We found that *nhr-49* is not required for the *C. elegans* immune defense against Bt on OP50. Additionally, neither MYb11-, nor MYb115-mediated protection against Bt infection was dependent on *nhr-49* (Figure 5B). This could indicate that FAT-7 acts independent of *nhr-49* in the context of MYb11.

Taken together, exposure to both *Pseudomonas* strains, MYb11 and MYb115, leads to diverging changes in the abundances of fat metabolism proteins independent of the fat metabolism regulator NHR-49. The role of the identified enzymes of the long-chain fatty acid synthesis pathway (e. g. FAT-7) in MYb11- and MYb115-mediated protection has yet to be defined.

## Intermediate filament IFB-2 is involved in MYb115-mediated protection against Bt247.

Another intriguing result of our overrepresentation analysis was the presence of cytoskeleton-related terms (e. g., GO:0007010, GO:0007071, GO:0000226) (Figure 3B, C). As our previous proteome dataset of *C. elegans* infected with *B. thuringiensis* similarly showed an enrichment in cytoskeleton-based GO terms (53, 68), we wondered whether systematic reorganization of the cytoskeleton evoked by microbiota members MYb11 and MYb115 might mediate defense against *Bt*. Therefore, we extracted all proteins of our proteome dataset with the GO term cytoskeleton (Table S3) and analyzed their abundance pattern (Figure 6A). Strikingly, four out of five intermediate filaments we identified in the overall analysis, IFB-2, IFP-1, and two IFA-1 isoforms, were more abundant in MYb115-treated worms compared to MYb11- or OP50-fed worms.

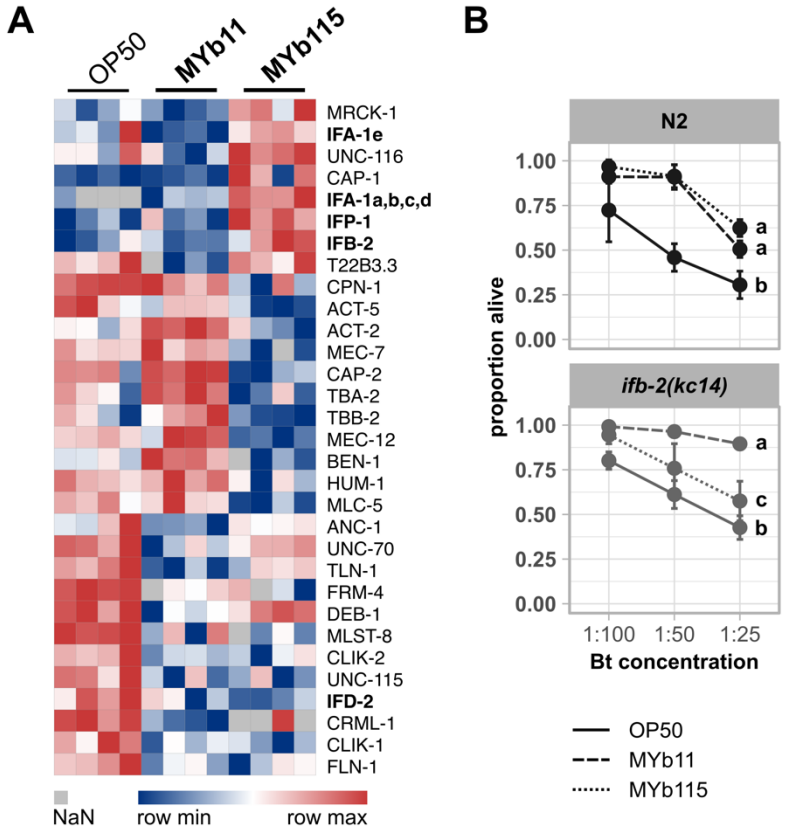


**Figure 6. IFB-2 is required for a full MYb115-mediated protective effect against Bt247 infection.** (A) Heatmap showing the $\log_2$ label-free intensity values of identified proteins related to the GO term cytoskeleton. The columns denote the bacterial treatment with 4 replicates each, each row represents one protein. (B) Survival of N2 and *ifb-2(kc14)* infected with serial dilutions of *B. thuringiensis* Bt247 after 24 hpi. Worms were exposed to either OP50, MYb11, or MYb115 before and during infection. Means ± standard deviation (SD) of n = 4 are shown. Same letters indicate no significant differences between the dose response curves according to a generalized linear model (GLM) (57) and Bonferroni correction. Corresponding *p*-values are provided in Table S7.

The cytoskeleton, consisting of actin-based microfilaments, tubulin-based microtubules, and intermediate filaments (69), canonically stabilizes and maintains the cellular shape ((70); reviewed in (71)). In the context of infection, the cytoskeleton also functions as a vital innate immune barrier against microbial intruders (reviewed in (72, 73)) but can equally be targeted and exploited by bacterial pathogens (reviewed in (74, 75)). For instance, the Bt pore-forming toxin Cry5B leads to structural alterations in the *C. elegans* intermediate filament-rich endotube and intermediate filament IFB-2 is required to withstand the detrimental impact of Cry5B (76). Furthermore, the *C. elegans* NCK-1 homolog to human Nck, an activator of actin assembly, was reported to be required for membrane repair after pore-forming toxin attack (77).

We thus examined the role of intermediate filament protein IFB-2 in MYb115-mediated protection against Bt infection. We found that the protective effect of MYb115 against Bt infection is indeed either partially (Figure 6B), or completely dependent on *ifb-2* in three out of four experiments (Figure S1). On the contrary, the MYb11-mediated protective effect seems to be independent of IFB-2 (in all three experiments; Figure 6B, Figure S1).

It is tempting to speculate that modulations in cytoskeleton dynamics, i. e. via an increase in intermediate filament protein production by MYb115, might enhance the integrity of the intestinal epithelium and thus contribute to defense against pathogens. It was reported that microbial-derived metabolites (e. g., propionate and butyrate) can lead to remodeling of the actin cytoskeleton and to an increase in tight junctions in an *in vitro* blood-brain-barrier model, thereby protecting against LPS-induced disturbances (78). Future research may further elucidate the impact of *P. fluorescens* MYb115 on the *C. elegans* intestinal cytoskeleton and its exact role in microbiota-mediated protection against Bt pore-forming toxins.

# Conclusion

We aimed to identify *C. elegans* proteins which partake in the interaction between the nematode host and two of its protective gut mutualists, *P. lurida* MYb11 and *P. fluorescens* MYb115. We identified proteins affected by both, MYb11 and MYb115, including vitellogenins and proteins involved in vitamin $B_{12}$-dependent metabolism, but also proteins more specifically affected by either Pseudomonads. The latter are of specific interest, since MYb11 and MYb115 protect *C. elegans* against *B. thuringiensis* infection by distinct mechanisms. We observed that MYb11 and MYb115 affect different proteins involved in fat metabolism. Also, we found higher abundances of candidate immune effector proteins in response to MYb11 and higher abundances of intermediate filament proteins in response to MYb115. We demonstrate that MYb115-mediated protection against infection with *B. thuringiensis* partially depends on the intermediate filament protein IFB-2. Thus, we provide evidence of increased host antimicrobial defenses by MYb11 and an influence of MYb115 on the cytoskeleton. Overall, this study expands our knowledge on microbiota-mediated effects on *C. elegans* physiology.

# Acknowledgments

We thank Lena Bluhm, Sabrina Butze, Laura Brügmann, Johanna Jarstorff, and Hanne Griem-Krey for technical support and the Schulenburg group for valuable feedback and discussions. We appreciate the services of the CGC, which is funded by NIH Office of Research Infrastructure Programs (P40 OD010440), for providing worm strains; the Leube Lab at RWTH Aachen, Germany, for providing the mutant *ifb-2(kc14)*, and SunyBiotech for generating transgenic strain F55G11.4p::gfp. This project was funded by the German Science Foundation DFG (Collaborative Research Center CRC 1182 Origin and Function of Metaorganisms, project A1.2 to KD and project Z3 to AT).


# Supplemental Materials

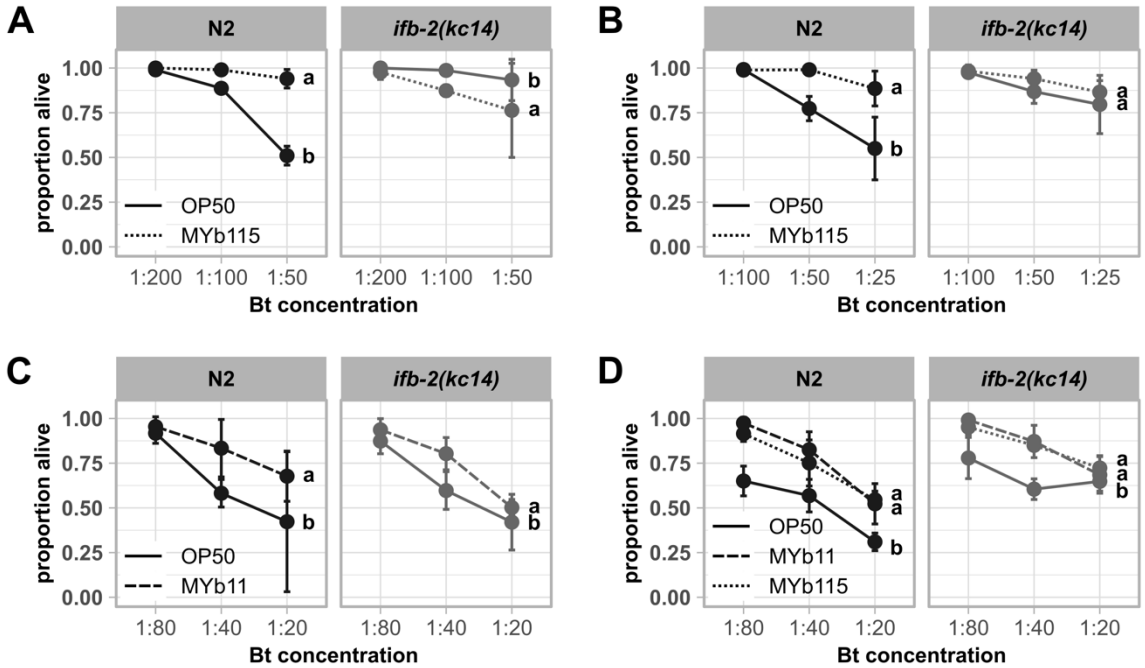


**Figure S1. IFB-2 is required for the MYb115-mediated protective effect against Bt247 infection.** Survival of N2 and *ifb-2(kc14)* infected with serial dilutions of *B. thuringiensis* Bt247 after 24 hpi. Worms were exposed to either OP50, MYb11, or MYb115 before and during infection. Means ± standard deviation (SD) of n = 3-4 are shown. Same letters indicate no significant differences between the dose response curves according to a generalized linear model (GLM) (57) and Bonferroni correction. Corresponding *p*-values are provided in Table S7.

**Table S1. Transgenic strains and mutants employed in this study.**

**Table S2. Primer sequences for qRT–PCRs.**

**Table S3. Raw data and statistical analyses of proteome dataset.**

**Table S4. Proteins commonly differentially abundant in C. elegans in response to microbiome members *Ochrobactrum* MYb71 and MYb237, and *Pseudomonas* MYb11 and MYb115.**

**Table S5. Significantly enriched gene ontology (GO) terms in cluster 1 and 4 (different abundances of proteins uniquely in MYb11-treated worms).**

**Table S6. Significantly enriched gene ontology (GO) terms in cluster 2 and 3 (different abundances of proteins uniquely in MYb115-treated worms).**

**Table S7. Raw data and statistical analyses of experiments.**

**Supplemental Materials and Methods**

# References


1. Zhang J, Holdorf AD, Walhout AJ. 2017. C. elegans and its bacterial diet as a model for systems-level understanding of host–microbiota interactions. Current Opinion in Biotechnology 46:74–80.

2. Roselli M, Schifano E, Guantario B, Zinno P, Uccelletti D, Devirgiliis C. 2019. *Caenorhabditis elegans* and probiotics interactions from a prolongevity perspective. 20. Int J Mol Sci 20:E5020.

3. Dirksen P, Marsh SA, Braker I, Heitland N, Wagner S, Nakad R, Mader S, Petersen C, Kowallik V, Rosenstiel P, Félix M-A, Schulenburg H. 2016. The native microbiome of the nematode *Caenorhabditis elegans*: gateway to a new host-microbiome model. BMC Biol 14:38.

4. Zhang F, Berg M, Dierking K, Félix M-A, Shapira M, Samuel BS, Schulenburg H. 2017. *Caenorhabditis elegans* as a model for microbiome research. Front Microbiol 8.

5. Dirksen P, Assié A, Zimmermann J, Zhang F, Tietje A-M, Marsh SA, Félix M-A, Shapira M, Kaleta C, Schulenburg H, Samuel B. 2020. CeMbio - The *Caenorhabditis elegans* microbiome resource. G3 g3.401309.2020.

6. Backes C, Martinez-Martinez D, Cabreiro F. 2021. *C. elegans*: A biosensor for host–microbe interactions. Lab Anim 50:127–135.

7. Berg M, Zhou XY, Shapira M. 2016. Host-specific functional significance of *Caenorhabditis* gut commensals. Front Microbiol 7.

8. Montalvo-Katz S, Huang H, Appel MD, Berg M, Shapira M. 2013. Association with soil bacteria enhances p38-dependent infection resistance in *Caenorhabditis elegans*. Infection and Immunity 81:514–520.

9. Kissoyan KAB, Drechsler M, Stange E-L, Zimmermann J, Kaleta C, Bode HB, Dierking K. 2019. Natural *C. elegans* microbiota protects against infection via production of a cyclic lipopeptide of the viscosin group. Current Biology 29:1030-1037.e5.

10. Kissoyan KAB, Peters L, Giez C, Michels J, Pees B, Hamerich IK, Schulenburg H, Dierking K. 2022. Exploring effects of *C. elegans* protective natural microbiota on host physiology. Front Cell Infect Microbiol 12:775728.

11. MacNeil LT, Watson E, Arda HE, Zhu LJ, Walhout AJM. 2013. Diet-induced developmental acceleration independent of TOR and insulin in *C. elegans*. Cell 153:240–252.

12. Yang W, Petersen C, Pees B, Zimmermann J, Waschina S, Dirksen P, Rosenstiel P, Tholey A, Leippe M, Dierking K, Kaleta C, Schulenburg H. 2019. The inducible response of the nematode *Caenorhabditis elegans* to members of its natural microbiota across development and adult life. Front Microbiol 10:1793.

13. Coolon JD, Jones KL, Todd TC, Carr BC, Herman MA. 2009. *Caenorhabditis elegans* genomic response to soil bacteria predicts environment-specific genetic effects on life history traits. 6. PLoS Genet 5:e1000503.

14. Goya ME, Xue F, Sampedro-Torres-Quevedo C, Arnaouteli S, Riquelme-Dominguez L, Romanowski A, Brydon J, Ball KL, Stanley-Wall NR, Doitsidou M. 2020. Probiotic *Bacillus subtilis* protects against α-synuclein aggregation in *C. elegans*. Cell Reports 30:367-380.e7.

15. Grishkevich V, Ben-Elazar S, Hashimshony T, Schott DH, Hunter CP, Yanai I. 2012. A genomic bias for genotype-environment interactions in *C. elegans*. Mol Syst Biol 8:587.

16. Cassidy L, Petersen C, Treitz C, Dierking K, Schulenburg H, Leippe M, Tholey A. 2018. The *Caenorhabditis* elegans proteome response to naturally associated microbiome members of the genus *Ochrobactrum*. PROTEOMICS 18:1700426.

17. Mørch MGM, Møller KV, Hesselager MO, Harders RH, Kidmose CL, Buhl T, Fuursted K, Bendixen E, Shen C, Christensen LG, Poulsen CH, Olsen A. 2021. The TGF-β ligand DBL-1 is a key player in a multifaceted probiotic protection against MRSA in C. elegans. Sci Rep 11:10717.

18. Stiernagle T. 2006. Maintenance of *C. elegans*. WormBook https://doi.org/10.1895/wormbook.1.101.1.

19. Borgonie G, Van Driessche R, Leyns F, Arnaut G, De Waele D, Coomans A. 1995. Germination of *Bacillus thuringiensis* spores in bacteriophagous nematodes (Nematoda: Rhabditida). Journal of Invertebrate Pathology 65:61–67.

20. Ou H-L, Kim CS, Uszkoreit S, Wickström SA, Schumacher B. 2019. Somatic niche cells regulate the CEP-1/p53-mediated DNA damage response in primordial germ cells. Developmental Cell 50:167-183.e8.

21. Livak KJ, Schmittgen TD. 2001. Analysis of relative gene expression data using real-time quantitative PCR and the $2^{-\Delta\Delta C_T}$ method. Methods 25:402–408.

22. Schneider CA. 2012. NIH Image to ImageJ: 25 years of image analysis. FOCUS ON BIOIMAGE INFORMATICS.

23. Hughes CS, Moggridge S, Müller T, Sorensen PH, Morin GB, Krijgsveld J. 2019. Single-pot, solid-phase-enhanced sample preparation for proteomics experiments. Nat Protoc 14:68–85.

24. Tyanova S, Cox J. 2018. Perseus: A bioinformatics platform for integrative analysis of proteomics data in cancer research, p. 133–148. *In* von Stechow, L (ed.), Cancer Systems Biology: Methods and Protocols. Springer New York, New York, NY.

25. Vizcaíno JA, Deutsch EW, Wang R, Csordas A, Reisinger F, Ríos D, Dianes JA, Sun Z, Farrah T, Bandeira N, Binz P-A, Xenarios I, Eisenacher M, Mayer G, Gatto L, Campos A, Chalkley RJ, Kraus H-J, Albar JP, Martinez-Bartolomé S, Apweiler R, Omenn GS, Martens L, Jones AR, Hermjakob H. 2014. ProteomeXchange provides globally coordinated proteomics data submission and dissemination. Nat Biotechnol 32:223–226.

26. Cheng X, Yan J, Liu Y, Wang J, Taubert S. 2021. eVITTA: a web-based visualization and inference toolbox for transcriptome analysis. Nucleic Acids Research 49:W207–W215.

27. Wickham H. 2016. ggplot2: Elegant graphics for data analysis. Springer-Verlag New York.

28. Blumenthal T, Squire M, Kirtland S, Cane J, Donegan M, Spieth J, Sharrock W. 1984. Cloning of a yolk protein gene family from *Caenorhabditis elegans*. Journal of Molecular Biology 174:1–18.

29. Spieth J, Blumenthal T. 1985. The *Caenorhabditis elegans* vitellogenin gene family includes a gene encoding a distantly related protein. Molecular and Cellular Biology 5:2495–2501.

30. Perez MF, Lehner B. 2019. Vitellogenins - Yolk gene function and regulation in *Caenorhabditis elegans*. Front Physiol 10:1067.

31. Van Nostrand EL, Sánchez-Blanco A, Wu B, Nguyen A, Kim SK. 2013. Roles of the developmental regulator *unc-62*/Homothorax in limiting longevity in *Caenorhabditis elegans*. PLoS Genet 9:e1003325.

32. Salmela H, Amdam GV, Freitak D. 2015. Transfer of immunity from mother to offspring is mediated via egg-yolk protein vitellogenin. PLoS Pathog 11:e1005015.

33. Fischer M, Regitz C, Kull R, Boll M, Wenzel U. 2013. Vitellogenins increase stress resistance of *Caenorhabditis elegans* after *Photorhabdus luminescens* infection depending on the steroid-signaling pathway. Microbes and Infection 15:569–578.

34. Zimmermann J, Obeng N, Yang W, Pees B, Petersen C, Waschina S, Kissoyan KA, Aidley J, Hoeppner MP, Bunk B, Spröer C, Leippe M, Dierking K, Kaleta C, Schulenburg H. 2020. The functional repertoire contained within the native microbiota of the model nematode *Caenorhabditis elegans*. ISME J 14:26–38.

35. Watson E, MacNeil LT, Ritter AD, Yilmaz LS, Rosebrock AP, Caudy AA, Walhout AJM. 2014. Interspecies systems biology uncovers metabolites affecting *C. elegans* gene expression and life history traits. Cell 156:759–770.

36. Giese GE, Walker MD, Ponomarova O, Zhang H, Li X, Minevich G, Walhout AJ. 2020. *Caenorhabditis elegans* methionine/S-adenosylmethionine cycle activity is sensed and adjusted by a nuclear hormone receptor. eLife 9:e60259.

37. Bender DA. 2003. Nutritional biochemistry of the vitamins, 2nd ed. Cambridge University Press, Cambridge. https://www.cambridge.org/core/books/nutritional-biochemistry-of-the-vitamins/10B31039A2B0F4B4DC58A89C523FAE97.

38. Bito T, Matsunaga Y, Yabuta Y, Kawano T, Watanabe F. 2013. Vitamin $B_{12}$ deficiency in *Caenorhabditis elegans* results in loss of fertility, extended life cycle, and reduced lifespan. FEBS Open Bio 3:112–117.

39. Revtovich AV, Lee R, Kirienko NV. 2019. Interplay between mitochondria and diet mediates pathogen and stress resistance in *Caenorhabditis elegans*. PLoS Genet 15:e1008011.

40. Watson E, Olin-Sandoval V, Hoy MJ, Li C-H, Louisse T, Yao V, Mori A, Holdorf AD, Troyanskaya OG, Ralser M, Walhout AJ. 2016. Metabolic network rewiring of propionate flux compensates vitamin $B_{12}$ deficiency in *C. elegans*. eLife 5:e17670.

41. Bulcha JT, Giese GE, Ali MdZ, Lee Y-U, Walker MD, Holdorf AD, Yilmaz LS, Brewster RC, Walhout AJM. 2019. A persistence detector for metabolic network rewiring in an animal. Cell Reports 26:460-468.e4.

42. Arda HE, Taubert S, MacNeil LT, Conine CC, Tsuda B, Van Gilst M, Sequerra R, Doucette-Stamm L, Yamamoto KR, Walhout AJM. 2010. Functional modularity of nuclear hormone receptors in a *Caenorhabditis elegans* metabolic gene regulatory network. Mol Syst Biol 6:367.

43. Winter AD, Tjahjono E, Beltrán LJ, Johnstone IL, Bulleid NJ, Page AP. 2022. Dietary-derived vitamin $B_{12}$ protects *Caenorhabditis elegans* from thiol-reducing agents. BMC Biol 20:228.

44. McDonagh A, Crew J, van der Linden AM. 2022. Dietary vitamin $B_{12}$ regulates chemosensory receptor gene expression via the MEF2 transcription factor in *Caenorhabditis elegans*. 6. G3 Genes|Genomes|Genetics 12:jkac107.

45. Nair T, Chakraborty R, Singh P, Rahman SS, Bhaskar AK, Sengupta S, Mukhopadhyay A. 2022. Adaptive capacity to dietary vitamin $B_{12}$ levels is maintained by a gene-diet interaction that ensures optimal life span. 1. Aging Cell 21:e13518.

46. Benedetti C, Haynes CM, Yang Y, Harding HP, Ron D. 2006. Ubiquitin-like protein 5 positively regulates chaperone gene expression in the mitochondrial unfolded protein response. Genetics 174:229–239.

47. Haynes CM, Petrova K, Benedetti C, Yang Y, Ron D. 2007. ClpP mediates activation of a mitochondrial unfolded protein response in *C. elegans*. Developmental Cell 13:467–480.

48. Leiers B, Kampkötter A, Grevelding CG, Link CD, Johnson TE, Henkle-Dührsen K. 2003. A stress-responsive glutathione S-transferase confers resistance to oxidative stress in *Caenorhabditis elegans*. Free Radical Biology and Medicine 34:1405–1415.

49. Estes KA, Dunbar TL, Powell JR, Ausubel FM, Troemel ER. 2010. bZIP transcription factor *zip-2* mediates an early response to *Pseudomonas aeruginosa* infection in *Caenorhabditis elegans*. Proc Natl Acad Sci USA 107:2153–2158.

50. Irazoqui JE, Ng A, Xavier RJ, Ausubel FM. 2008. Role for β-catenin and HOX transcription factors in *Caenorhabditis elegans* and mammalian host epithelial-pathogen interactions. Proc Natl Acad Sci USA 105:17469–17474.

51. Samuel BS, Rowedder H, Braendle C, Félix M-A, Ruvkun G. 2016. *Caenorhabditis elegans* responses to bacteria from its natural habitats. Proc Natl Acad Sci USA 113:E3941–E3949.

52. Liu Y, Sellegounder D, Sun J. 2016. Neuronal GPCR OCTR-1 regulates innate immunity by controlling protein synthesis in *Caenorhabditis elegans*. Sci Rep 6:36832.

53. Treitz C, Cassidy L, Höckendorf A, Leippe M, Tholey A. 2015. Quantitative proteome analysis of *Caenorhabditis elegans* upon exposure to nematicidal *Bacillus thuringiensis*. Journal of Proteomics 113:337–350.

54. Boehnisch C, Wong D, Habig M, Isermann K, Michiels NK, Roeder T, May RC, Schulenburg H. 2011. Protist-type lysozymes of the nematode *Caenorhabditis elegans* contribute to Resistance against pathogenic *Bacillus thuringiensis*. PLoS ONE 6:e24619.

55. Ideo H, Fukushima K, Gengyo-Ando K, Mitani S, Dejima K, Nomura K, Yamashita K. 2009. A *Caenorhabditis elegans* glycolipid-binding galectin functions in host defense against bacterial infection. Journal of Biological Chemistry 284:26493–26501.

56. Pees B, Yang W, Kloock A, Petersen C, Peters L, Fan L, Friedrichsen M, Butze S, Zárate-Potes A, Schulenburg H, Dierking K. 2021. Effector and regulator: Diverse functions of *C. elegans* C-type lectin-like domain proteins. PLoS Pathog 17:e1009454.

57. Nelder JA, Wedderburn RWM. 1972. Generalized linear models. Journal of the Royal Statistical Society Series A (General) 135:370.

58. Kim Y, Mylonakis E. 2012. *Caenorhabditis elegans* immune conditioning with the probiotic bacterium *Lactobacillus acidophilus* strain NCFM enhances Gram-positive immune responses. Infect Immun 80:2500–2508.

59. Sang Y, Ren J, Aballay A. 2022. The transcription factor HLH-26 controls probiotic-mediated protection against intestinal infection through up-regulation of the Wnt/BAR-1 pathway. PLoS Biol 20:e3001581.

60. Irazoqui JE, Troemel ER, Feinbaum RL, Luhachack LG, Cezairliyan BO, Ausubel FM. 2010. Distinct pathogenesis and host responses during infection of *C. elegans* by *P. aeruginosa* and *S. aureus*. PLoS Pathog 6:e1000982.

61. Singh J, Aballay A. 2019. Intestinal infection regulates behavior and learning via neuroendocrine signaling. eLife 8:e50033.

62. Dasgupta M, Shashikanth M, Gupta A, Sandhu A, De A, Javed S, Singh V. 2020. NHR-49 transcription factor regulates immunometabolic response and survival of *Caenorhabditis elegans* during *Enterococcus faecalis* infection. Infect Immun 88:e00130-20.

63. Anderson SM, Cheesman HK, Peterson ND, Salisbury JE, Soukas AA, Pukkila-Worley R. 2019. The fatty acid oleate is required for innate immune activation and pathogen defense in *Caenorhabditis elegans*. PLoS Pathog 15:e1007893.

64. Watts JL, Browse J. 2000. A palmitoyl-CoA-specific Δ9 fatty acid desaturase from <i>Caenorhabditis elegans<i/>. Biochemical and Biophysical Research Communications 272:263–269.

65. Gilst MRV, Hadjivassiliou H, Jolly A, Yamamoto KR. 2005. Nuclear hormone receptor NHR-49 controls fat consumption and fatty acid composition in <i>C. elegans<i/>. PLoS Biol 3:e53.

66. Naim N, Amrit FRG, Ratnappan R, DelBuono N, Loose JA, Ghazi A. 2021. Cell nonautonomous roles of NHR-49 in promoting longevity and innate immunity. Aging Cell 20.

67. Wani KA, Goswamy D, Taubert S, Ratnappan R, Ghazi A, Irazoqui JE. 2021. NHR-49/PPAR-α and HLH-30/TFEB cooperate for *C. elegans* host defense via a flavin-containing monooxygenase. eLife 10:e62775.

68. Yang W, Dierking K, Esser D, Tholey A, Leippe M, Rosenstiel P, Schulenburg H. 2015. Overlapping and unique signatures in the proteomic and transcriptomic responses of the nematode *Caenorhabditis elegans* toward pathogenic *Bacillus thuringiensis*. Developmental & Comparative Immunology 51:1–9.

69. Carberry K, Wiesenfahrt T, Windoffer R, Bossinger O, Leube RE. 2009. Intermediate filaments in *Caenorhabditis elegans*. Cell Motil Cytoskeleton 66:852–864.

70. Alberts B, Bray D, Hopkin K, Johnson AD, Lewis J, Raff M, Roberts K, Walter P. 2013. Essential cell biology, 4th ed. Garland Publishing.

71. Coch R, Leube R. 2016. Intermediate filaments and polarization in the intestinal epithelium. Cells 5:32.

72. Geisler F, Leube R. 2016. Epithelial intermediate filaments: guardians against microbial infection? Cells 5:29.

73. Mostowy S, Shenoy AR. 2015. The cytoskeleton in cell-autonomous immunity: structural determinants of host defence. Nat Rev Immunol 15:559–573.

74. Dramsi S, Cossart P. 1998. Intracellular pathogens and the actin cytoskeleton. Annual Review of Cell and Developmental Biology 14:137–66.

75. Bhavsar AP, Guttman JA, Finlay BB. 2007. Manipulation of host-cell pathways by bacterial pathogens. Nature 449:827–834.

76. Geisler F, Coch RA, Richardson C, Goldberg M, Denecke B, Bossinger O, Leube RE. 2019. The intestinal intermediate filament network responds to and protects against microbial insults and toxins. Development dev.169482.

77. Sitaram A, Yin Y, Zamaitis T, Zhang B, Aroian RV. 2022. A *Caenorhabditis elegans nck-1* and filamentous actin-regulating protein pathway mediates a key cellular defense against bacterial pore-forming proteins. PLoS Pathog 18:e1010656.

78. Knox EG, Aburto MR, Tessier C, Nagpal J, Clarke G, O'Driscoll CM, Cryan JF. 2022. Microbial-derived metabolites induce actin cytoskeletal rearrangement and protect blood-brain barrier function. iScience 25:105648.